



Stratification of microbiomes during the holomictic period of Lake Fuxian, an alpine monomictic lake

Peng Xing ^{1*}, Ye Tao,^{1,2} Jianhua Luo,^{1,3} Lina Wang,^{1,2} Biao Li,^{1,2} Huabing Li,¹ Qinglong L. Wu ^{1,3*}

¹State Key Laboratory of Lake Science and Environment, Nanjing Institute of Geography and Limnology, Chinese Academy of Sciences, Nanjing, China

²University of Chinese Academy of Sciences, Beijing, China

³Sino-Danish Centre for Education and Research, University of Chinese Academy of Sciences, Beijing, China

Abstract

In warm monomictic lakes, the hypolimnion is important for accumulating and decomposing organic matter derived from surface production, and the regenerated nutrients will be supplied to the epilimnion through winter vertical mixing. So far, we know little about microbial community composition and function in the hypolimnion when the significant thermal stratification disappears. In this study, we investigated microbial community compositions and functional gene contents by means of metagenomics along a depth profile in the warm monomictic alpine Lake Fuxian during holomictic period. Overall, bacteria were the dominant microbial group at different water depths, while phages had their high relative abundance in the epilimnion. We observed slight thermal but strong chemical stratification even during this typical winter overturn. The anaerobic respiration with nitrate and sulfate as the terminal electron acceptors was accumulated at bottom of hypolimnion as indicated through metabolic pathway reconstruction. We were able to get 440 metagenome-assembled genomes (MAGs) and unraveled a high genomic diversity of freshwater pelagic microbiomes along this depth profile. We furthermore defined a new class of “Plancto_FXH1” of *Planctomycetes* from these MAGs, of which a distinct nitrate reduction operon was identified. Representatives of this phylum mainly thrive in the hypolimnion as previously suspected, but few lineages were detected in the epilimnion. In summary, metagenomics enabled us to find a new group of *Planctomycetes*, probably involved in denitrification in the hypolimnion in Lake Fuxian, which expand our knowledge on denitrifying bacterial diversity and their denitrification potential in deep freshwater lakes.

Warm monomictic lakes never freeze and are thermally stratified throughout much of the year. The density difference between the warm surface waters (the epilimnion) and the colder bottom waters (the hypolimnion) prevents these lakes from mixing in summer, whereas in winter, the surface waters cool to a temperature equal to that of the bottom waters. Such lakes are widely distributed from temperate to tropical regions (Lewis 1983).

Deep-water winter oxygenation in warm monomictic lakes is vital to the function of lake ecosystems, the lack of which may threaten benthic fauna (Rabalais et al. 2001) and alter

biogeochemical cycles (Wetzel 2001). The microorganisms inhabiting the hypolimnion are responsible for accumulating and decomposing organic matter derived from surface production. The regenerated nutrients will be supplied to the epilimnion through winter vertical mixing. It should be noted that the current climate change model is not optimistic for the scenario of thorough mixing in deep lakes, with studies indicating that the ongoing trend of climate warming (Livingstone 2003) may lead to year-round oxygen depletion in deep water within a half century (Danis et al. 2004; Matzinger et al. 2007). Moreover, prolonged stable stratification may be accompanied by increases in hypolimnetic phosphorous concentrations and increased phytoplankton abundances in subsequent years (Lindström et al. 2004; Lavoie and Auclair 2012). The metabolism of organic matter derived from the epilimnion increases oxygen demand, which further deteriorates hypolimnetic oxygen conditions (Naeher et al. 2013). Studies have demonstrated that the ecosystem and biogeochemical cycling in oxygenated hypolimnia are driven by a specific bacterial community that is considerably different from that present in epilimnia (Okazaki and Nakano 2016; Okazaki et al. 2017; Linz et al. 2017). We speculated

*Correspondence: qlwu@niglas.ac.cn (Q.L.W.) or pxing@niglas.ac.cn (P.X.)

This is an open access article under the terms of the Creative Commons Attribution License, which permits use, distribution and reproduction in any medium, provided the original work is properly cited.

Additional Supporting Information may be found in the online version of this article.

Special Issue: Linking metagenomics to Aquatic Microbial Ecology and Biogeochemical Cycles. Edited by: Hans-Peter Grossart, Ramon Massana, Katherine McMahon and David A. Walsh.

that oxygen-independent biogeochemical cycling would be predominant in the hypolimnion when oxygen supply was insufficient during the winter holomictic period.

The diversified niches in deep lakes may provide an ideal habitat for the study of speciation and evolution of microbial linkages, especially those “less abundant phyla.” In recent years, a combination of improved cultivation techniques and the use of cultivation-independent approaches has led to an increasingly detailed understanding of several groups of abundant and ubiquitous freshwater microbes (Sorokin et al. 2012; Deneff et al. 2015; He et al. 2017; Henson et al. 2018; Mehrshad et al. 2018; Neuenschwander et al. 2018; Okazaki et al. 2018). Moreover, ecogenomic approaches have been used to unravel the evolutionary history for some hallmark freshwater lineages (Andrei et al. 2019). Processes involved in altering genomic architecture promoted the transition of sediment/soil-dwelling *Planctomycetes* into aquatic environments and gave rise to new habitat-specific lineages (e.g., lacustrine-specific). This transition has been well corroborated by the phylogenetic reconstructions of other abundant freshwater bacterial lineages, that is, *Betaproteobacteria* and *Verucomicrobia* (Salcher et al. 2015; Cabello-Yeves et al. 2017). Thus, we expected that deep lakes with a longer water retention time would harbor more habitat-specific lineages of microbes that are specialized to consume relatively recalcitrant dissolved organic matter, especially in the deep hypolimnion.

In this study, Lake Fuxian was taken as a model system to determine whether the annual physical mixing of water can blur the boundaries between epilimnetic and hypolimnetic microbiomes, which promote the development of uniform structure and function in the warm alpine region. Lake Fuxian (24°35'N, 102°50'E, 1788.5 m a.s.l.) is warm, oligotrophic monomictic lake located on the Yunnan-Guizhou Plateau and is the third deepest lake in China (maximum depth of 158.9 m, detailed information in Supporting Information Table S1) (Wang and Dou 1998). The water volume of Lake Fuxian is ca. 20.6 billion cubic meters, ranking first in freshwater lakes in China. This lake was formed by tectonic faulting, supposedly during Pliocene age. Field sampling was performed during the “theoretical” complete mixing period. Metagenomic deep sequencing was applied to systematically describe the depth profile of microbiomes. Relative gene abundance was used as a proxy for the in situ significance of several core metabolic pathways, which facilitated vertical comparisons among multiple depths.

Methods

Sample collection and measurements of environmental parameters

Water samples were collected from Lake Fuxian at the site of maximal depth (24°32'29"N, 102°53'41"E) with 3.5 L × 6 Multi Water Sampler (Slimline, HYDRO-BIOS, Germany) on

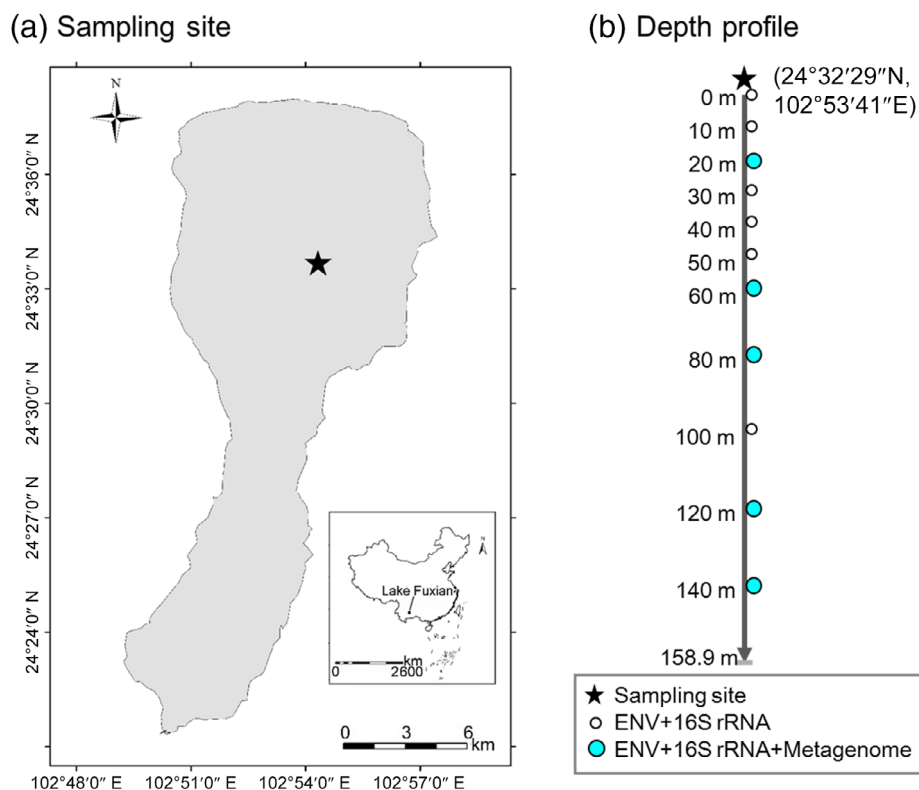


Fig. 1. Sampling strategies at the maximum depth of Lake Fuxian. **(a)** Sampling site; **(b)** Depth for different analyses are indicated: environmental factors (ENV), 16S rRNA gene amplicon sequencing (16S rRNA), and metagenomic sequencing (metagenome).

25 December 2017 (Fig. 1) from the water surface (0 m) down to a depth of 140 m, with samples collected also at 10, 20, 30, 40, 50, 60, 80, 100, and 120 m. The conductivity (Cond), pH, water temperature (Temp), and dissolved oxygen (DO) concentration were logged at 5 m intervals along the depth profile using a Multi-Parameter Water Quality Sonde (YSI 6600, Yellow Springs, U.S.A.). Water from each depth was prefiltered through a 200- μ m nylon mesh in the field and stored in 25-liter polycarbonate carboys until further processing in the laboratory 2–4 h later. Subsequently, 600 mL of water from each depth was filtered through 0.2- μ m polycarbonate membranes (Isopore™ Membrane Filters, Merck Millipore, U.S.A.) for bacterial diversity analysis. At least 15 liters of water (depths: 20, 60, 80, 120, and 140 m) was filtered by sequential filtration through 20- μ m pre-filters onto 3.0-, 0.8-, and 0.1- μ m filters (Isopore™ Membrane Filters, Merck Millipore) for metagenomic analyses (Ng et al. 2010). All of the filter membranes were flash-frozen in liquid-nitrogen and stored at -80°C . The concentrations of total phosphorus (TP), total nitrogen (TN), dissolved organic carbon (DOC), ammonium ($\text{NH}_4\text{-N}$), nitrate ($\text{NO}_3\text{-N}$), nitrite ($\text{NO}_2\text{-N}$), soluble phosphorus ($\text{PO}_4\text{-P}$), and chlorophyll *a* (Chl *a*) were measured using standard methods (Greenberg et al. 1992).

DNA extraction, library preparation, sequencing, and raw data processing

Microbial DNA was extracted from the filters using an E.Z.N.A.® water DNA kit (Omega Biotek, Norcross, U.S.A.) according to the manufacturer's protocols. Bacterial 16S rRNA gene amplification, sequencing and data processing are available in Supporting Information in the online version of the paper. Metagenomic shotgun sequencing libraries were constructed and sequenced at Shanghai Biozon Biological Technology. For each sample, 1 μ g of genomic DNA was sheared with a Covaris S220 Focused-ultrasonicator (Woburn, U.S.A.), and an average fragment length of approximately 450 bp was used to prepare the libraries. All of the samples were sequenced on an Illumina HiSeq X system using the paired-end 150 bp (PE150) mode. Raw sequence reads underwent quality trimming using Trimmomatic to remove adaptor contaminants and low-quality reads (Bolger et al. 2014). Reads that passed quality control were subsequently mapped against the human genome (version: hg19) and known nonenvironmental bacteria genomes (i.e., *Bradyrhizobium*, *Escherichia*, *Klebsiella*, and *Propionibacterium*; only complete genomes in the National Center for Biotechnology Information [NCBI] RefSeq release number: 90 was used in this study) using the BWA-MEM algorithm (parameters: `-M -k 32 -t 16`, <http://biobwa.sourceforge.net/bwa.shtml>). Finally, uncontaminated high-quality reads were called clean reads and used for subsequent analysis.

Phylogenetic annotation

Taxonomic assignments for the clean reads were made using a customized database that included the genome sequences of bacteria, archaea, fungi, viruses, protozoa, and algae in the

NCBI RefSeq database (release number: 90) via Kraken2 (Wood and Salzberg 2014). All of the reads were classified at seven phylogenetic levels (domain, phylum, class, order, family, genus, and species) or unclassified. The abundances of the taxonomic groups were estimated using Bracken, which can produce accurate species- and genus-level abundances, even for multiple near-identical species (Lu et al. 2017).

Metagenomic de novo assembly, gene prediction, and annotation

Clean sequence reads were used to generate a set of contigs for each sample using MegaHit with the parameters “-min-contig-len 500” (Li et al. 2016). Open reading frames (ORFs) in the assembled contigs were predicted using Prodigal v2.6.3 (Hyatt et al. 2012). All ORFs were used to generate a set of unique genes after clustering by CD-HIT (parameters: `-n 9 -c 0.95 -G 0 -M 0 -d 0 -a S 0.9 -r 1`, Fu et al. 2012). The longest sequence in each cluster was considered to be the representative sequence for each gene in each unique gene set. The abundance of each gene within a sample was calculated by using SOAPaligner (<https://github.com/ShujiaHuang/SOAPaligner>) and the following formulas:

$$\text{Ab}(S) = \text{Ab}(U) + \text{Ab}(M) \quad (1)$$

$$\text{Ab}(U) = \sum_{i=1}^M 1/l \quad (2)$$

$$\text{Ab}(M) = \sum_{i=1}^M (\text{Co} * 1) / l \quad (3)$$

where $\text{Ab}(S)$ represents gene abundance; $\text{Ab}(U)$ represents single-mapping read abundance; $\text{Ab}(M)$ represents multi-mapping read abundance; and l represents the length of a gene sequence. For each multiple read, there is a species-specific coefficient Co ; let us suppose one read in $\{M\}$ has alignments with N different species, then Co was calculated as follows:

$$\text{Co} = \frac{\text{Ab}(U)}{\sum_{i=1}^N \text{Ab}(U_i)} \quad (4)$$

We queried the unique gene set of each depth for protein-coding genes based on their assigned identifiers. GhostKOALA tool with GHOSTX searching against a nonredundant set of Kyoto Encyclopaedia of Genes and Genomes (KEGG) GENES was used to assign KEGG Orthology (KO) numbers to each gene in the unique gene set (default parameters; `genus_prokaryotes + family_eukaryotes + viruses`, Kanehisa et al. 2016). To quantify and compare the abundance of genes involved in carbon, nitrogen, and sulfur cycles, the relative abundance of the detected functional genes was summarized as a proxy of the potential relevance of each pathway in situ.

Metagenome-assembled genomes reconstruction

Metagenome-assembled genomes (MAGs) were constructed for each sample using the following pipeline. (1) Three

binning software applications, namely, metaBAT2 (Kang et al. 2015), MaxBin2 (Wu et al. 2014), and CONCOCT (Alneberg et al. 2014) were separately used to perform binning. The final refined bins were obtained using binning-refiner to improve the quality (Song and Thomas 2017). (2) The completeness and contamination of all of the bins was checked using CheckM v.1.0.3 (Parks et al. 2015). Bins with a completeness $\geq 50\%$ and contamination $\leq 10\%$ were considered to be “high quality” and were used in the subsequent analyses. (3) The raw abundance (A_j) of a specific bin in a given sample j was calculated using metaWRAP (Uritskiy et al. 2018) with the following formula:

$$A_j = \frac{\sum_{i=1}^N l_i c_{ij}}{\sum_{i=1}^N l_i} \quad (5)$$

The production length of contig (l_i) and its coverage (c_{ij}) in sample j was summed across all of the contigs (N) assigned to the bin and then divided by total length of the bin genome. (4) The average nucleotide identity (ANI) between each pair of bins was calculated using the OAT java script (<http://www.ezbiocloud.net/sw/oat>) for all of the bins. The bin pairs with $> 95\%$ ANI were considered to be the same species in the redundancy step. (5) The phylogenetic annotation of bins was generated using CheckM, where the most similar phylogenetic level of bins was indicated by the comparison between genes of the bins and each set of single copy genes at different phylogenetic levels. (6) All of the genes in a bin were transformed to protein sequences to generate the proteomes for each bin to reconstruct the phylogenetic tree using PhyloPhlan (Segata et al. 2013). (7) 16S rRNA genes within each high-quality bin were predicted using RNAmmer-1.2 (Lagesen et al. 2007). (8) The phylogenetic tree of 16S rRNA gene sequences was constructed using the maximum likelihood method based on the Kimura 2-parameter distance mode (Kimura 1980) in MEGA 7.0 (Kumar et al. 2016). In addition, to detect the viral elements at the contig level, VirSorter was used to extract the viral signal from all of the assemblies (Roux et al. 2015).

Functional potential annotation of MAGs

To get an insight on the functional features encoded in the 161 MAGs with completeness $\geq 80\%$ and contamination $\leq 10\%$, amino acidic sequences predicted by Prodigal v2.6.3 were used as input to EggNOG-mapper to infer functional features based on orthology prediction (Huerta-Cepas et al. 2017). The output file included the annotations for each protein based on Clusters of Orthologous Groups (COG) categories. The abundance of each COG category within a MAG was normalized by the summary of total proteins.

Statistical analysis

Correlation of functional genes and microbial taxa as well with the major environmental factors was analyzed using the R package “Hmisc” (method = “Pearson”). The correlation matrix was reordered according to the Pearson correlation

coefficient using the “hclust” method. The R packages “corplot” and “pheatmap” were used to generate heatmaps. Non-metric multidimensional scaling (NMDS) analysis was applied to the normalized COG categories of the 161 MAGs, with pairwise cluster distances calculated using Bray-Curtis dissimilarities. The NMDS analysis was performed using the function “metaMDS” in the R package vegan (v.2.2-0), with the number of dimensions set to four after manual inspection of scree plots. Welch’s t -test was used to test the hypothesis that two groups of *Planctomyces* MAGs have equal means of guanine-cytosine (GC) content, genome size, and COG categories.

Sequence data submission

All metagenomic sequence data produced during the study are deposited in the NCBI Sequence Read Archive (SRA) database. All MAGs used in this study can be accessed under the Bioproject PRJNA531348 via the accession numbers SXGV00000000-SYPR00000000.

Results

Environmental profile along the depth profile in Lake Fuxian

Although our sampling time in December is regarded as typical winter overturn period of Lake Fuxian, we still observed slight stratification of water temperature, which from the surface to the 50 m was predominantly homogenous, but from 50 m to the bottom there was still a ca. 2°C difference (Fig. 2a). Typically we found quick decrease of DO along the depth profile below 50 m, where the DO was 1.0 mg L^{-1} at a depth of 100 m and below 0.2 mg L^{-1} at the bottom. In this context, we defined 50 m as the boundary between the epilimnion and the hypolimnion during the holomictic period.

We also found high concentrations of $\text{PO}_4\text{-P}$, TP, and $\text{NO}_3\text{-N}$ but low concentrations of DOC and $\text{NH}_4\text{-N}$ in the hyperlimnion (Fig. 2b,c). Based on the correlation analysis between each pair of environmental factors, two groups of environmental factors were formed, one of which included factors such as $\text{PO}_4\text{-P}$, $\text{NO}_3\text{-N}$, TP, and Chl a , which was defined as ‘Depth + ENV’; the other group included the factors DO, DOC, Temp, pH, and $\text{NH}_4\text{-N}$, which was defined as ‘Depth – ENV’ (Supporting Information Fig. S1).

Microbial community composition along the water depth Overview

The metagenomic data set comprised ca. 286 million reads per sample with average length 377 bp. 31.24% of the metagenomic reads were taxonomically assigned based on the analysis pipeline (Table 1). More than 90% of all taxonomically assigned metagenomic reads matched bacteria (90.4–95.6%), with a few representatives observed from archaea (1.19–6.50%), eukaryotes (2.5–4.1%), and phages (0.05–0.47%) (Fig. 3a). Bacteria numerically dominated the genetic composition of the microbial communities, both at the aerobic epilimnion and the oxygen-deficient deep hypolimnion. Archaea were more

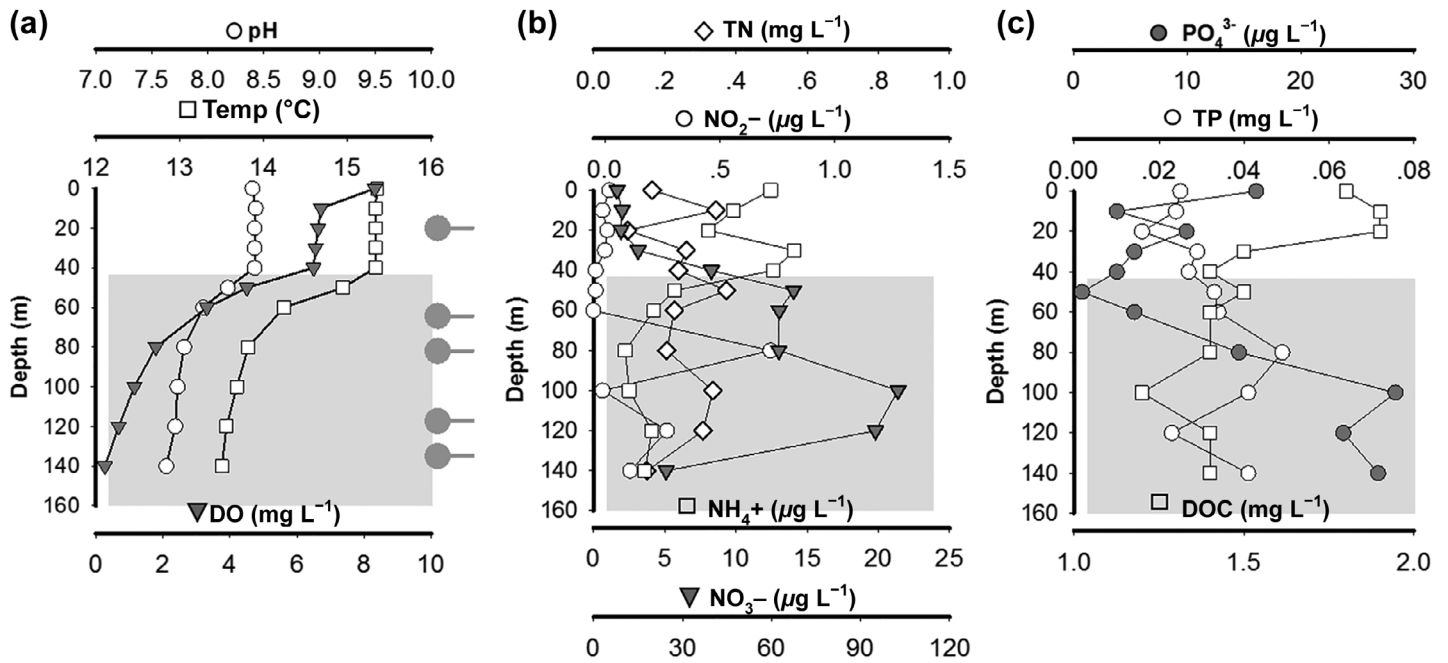


Fig. 2. Vertical profiles of physicochemical data at the Lake Fuxian sampling site. (a) Temp (open square), pH (open circle), and DO (filled down triangle); (b) TN (open diamond), NO_2^- (open circle), NH_4^+ (open square), and NO_3^- (filled down triangle); (c) PO_4^{3-} (filled circle), TP (open circle), and DOC (open square). Grey point at the right side of (a) indicated the water depth for metagenomic sequencing. Grey shade was used to discriminate hypolimnion from epilimnion.

abundant at a depth of 60 m, below the epilimnion-hypolimnion interface (6.50% of total reads), than at the epilimnion (1.19% of total reads) or hypolimnion (3.01% \pm 0.47%). With respect to the GC content of the clean metagenomic reads, increasing GC content of microbiomes was observed along the depth profile (Supporting Information Fig. S2).

Bacteria

Overall, the most abundant bacterial taxa recovered from the metagenomic data set matched *Proteobacteria* (average of 50.68%, range 44.60–58.17%), followed by *Actinobacteria* (29.37%, range 21.42–37.51%), *Acidobacteria* (4.67%, range 3.06–6.07%), *Firmicutes* (3.90%, range 2.82–4.87%), *Bacteroidetes* (3.75%, range 2.77–4.60%), *Planctomycetes* (2.00%, range 0.76–3.14%),

Nitrospirae (1.49%, range 0.12–2.42%), and other less abundant phyla (Supporting Information Fig. S3). At the class level, *Actinobacteria* were detected at abundant levels throughout in the water column, followed by *Alphaproteobacteria* (19.79%, range 17.78–23.12%), *Betaproteobacteria* (16.46%, range 13.36–22.07%), and *Gammaproteobacteria* (11.13%, range 7.72–13.65%) (Fig. 2b). The abundance of *Gammaproteobacteria* increased along the depth profile, showing a significantly negative correlation with the 'Depth - ENV' factor. In addition, *Deltaproteobacteria* were sensitive to TN and $\text{NO}_3\text{-N}$ variation.

Archaea

The major archaeal reads were affiliated with phylum *Thaumarchaeota* (average 67.3%), followed by *Euryarchaeota*

Table 1. Total number of metagenomic reads (averaged ca. 286 million per sample) for Lake Fuxian.

	20 m	60 m	80 m	120 m	140 m
The total number of raw reads	469,964,026	410,147,504	388,746,696	556,564,756	360,879,448
The total number of clean reads	292,321,532	286,255,246	251,912,634	349,465,112	249,988,154
Taxonomically assigned reads %	28.12	28.84	32.37	33.80	33.05
Functional aligned reads %	17.26	21.42	20.69	20.96	21.85
Bacteria %	94.27	90.37	93.61	95.59	93.73
Archaea %	1.19	6.50	3.62	1.84	3.55
Phages %	0.47	0.06	0.05	0.06	0.07
Fungi %	1.39	1.20	1.19	1.09	0.96
Apicomplexa %	0.42	0.16	0.15	0.13	0.15
Algae %	2.26	1.71	1.38	1.29	1.55

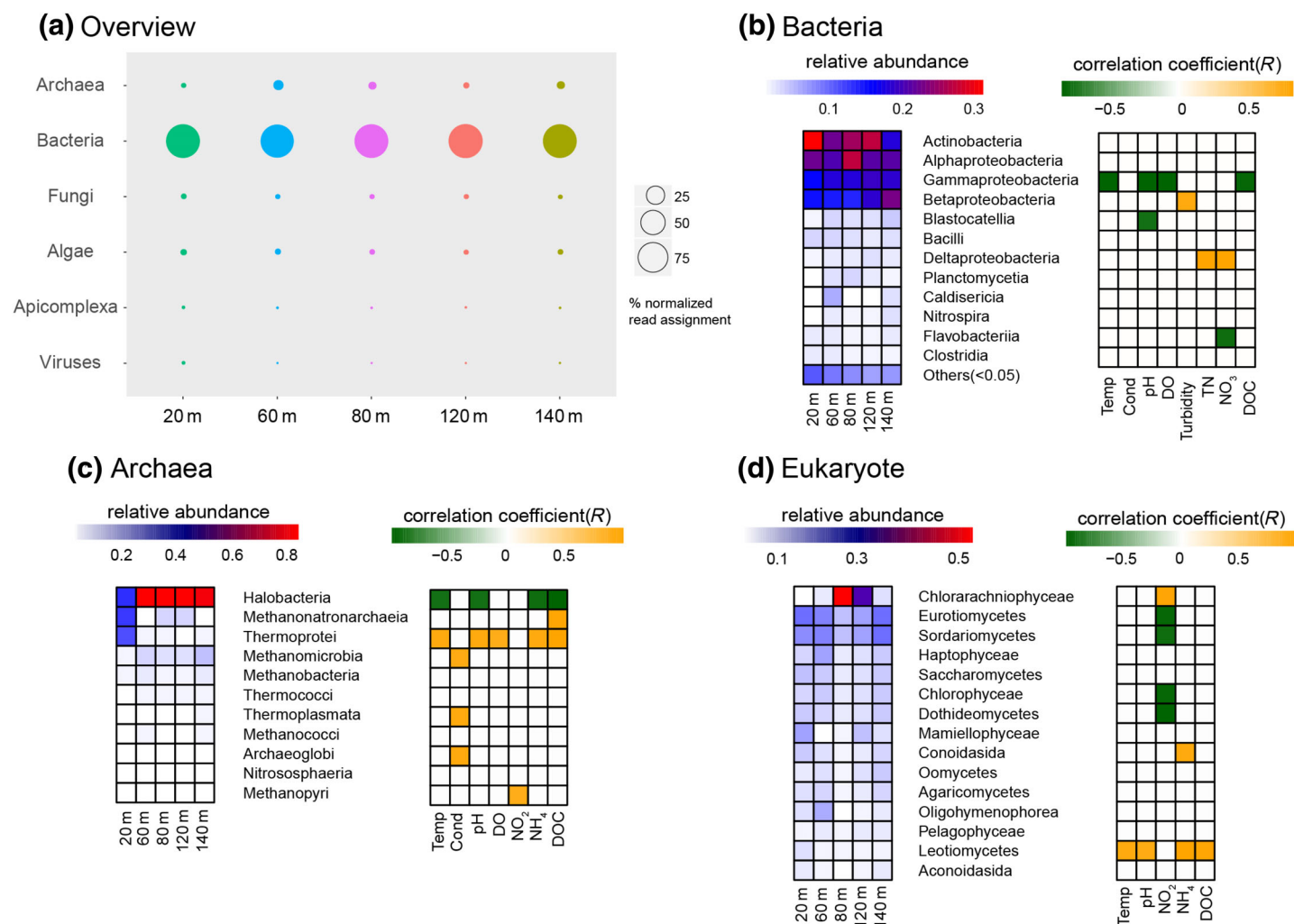


Fig. 3. Vertical profile of bacteria, archaea, and eukaryotes based on the taxonomy of the metagenomic reads. **(a)** Overview of the relative abundance of each domain; **(b)** dominant bacterial classes ($> 10^{-3}$ of normalized read assignments) and their response to environmental factors (Pearson correlation $|R| > 0.8$ and $p < 0.05$); **(c)** all archaeal classes; and **(d)** TOP15 eukaryotic classes.

(average 26.0%), *Candidatus Micrarchaeota* (average 6.2%), and few additional representatives of *Crenarchaeota* and *Candidatus Korarchaeota*. *Candidatus Micrarchaeota* was only detected in abundance at a depth of 20 m, whereas *Thaumarchaeota* was more abundant below epilimnion (Supporting Information Fig. S3). At the class level, *Halobacteria* were extremely predominant below the epilimnion (relative abundance of ca. 80%, Fig. 3c). In contrast, the relative abundances of *Thermoprotei* (29.33%) and *Methanonatronarchaeia* (29.87%) were ca. 15- and 600-fold higher in the epilimnion than in the deep hypolimnion, respectively. The abundance of *Halobacteria* exhibited a negative correlation with the 'Depth – ENV' factor, whereas the relative abundance of *Thermoprotei* with 'Depth – ENV' showed the opposite trend.

Eukaryotes

Algae became the most abundant Eukaryotes along the depth profile (average 1.64%, range 1.29–2.26% of all metagenomic

reads) after the prefiltration with the 20- μ m mesh, followed by fungi (1.17%, range 0.96–1.39%) and apicomplex (0.20%, range 0.13%–0.42%). Class *Chlorarachniophyceae* was the dominant eukaryotes, with maximum abundance at a depth of 80 m. Eukaryotes below a size of 20 μ m has less of a correlation with environmental fluctuations (Fig. 3d).

Phages

The maximum number of complete phages occurred at a depth of 20 m ($n = 923$), decreasing to 203 at a depth of 140 m. Most phages had no classification based on the current annotation pipeline. The uncultured Mediterranean phages (e.g., uvMED, uvDeep, and MEDS5) dominated the assigned phages, followed by *Synechococcus* phage, *Methylophilales* phage, and Cyanophage (Supporting Information Fig. S5). *Wolbachia* phage was only detected in the epilimnion with low abundance.

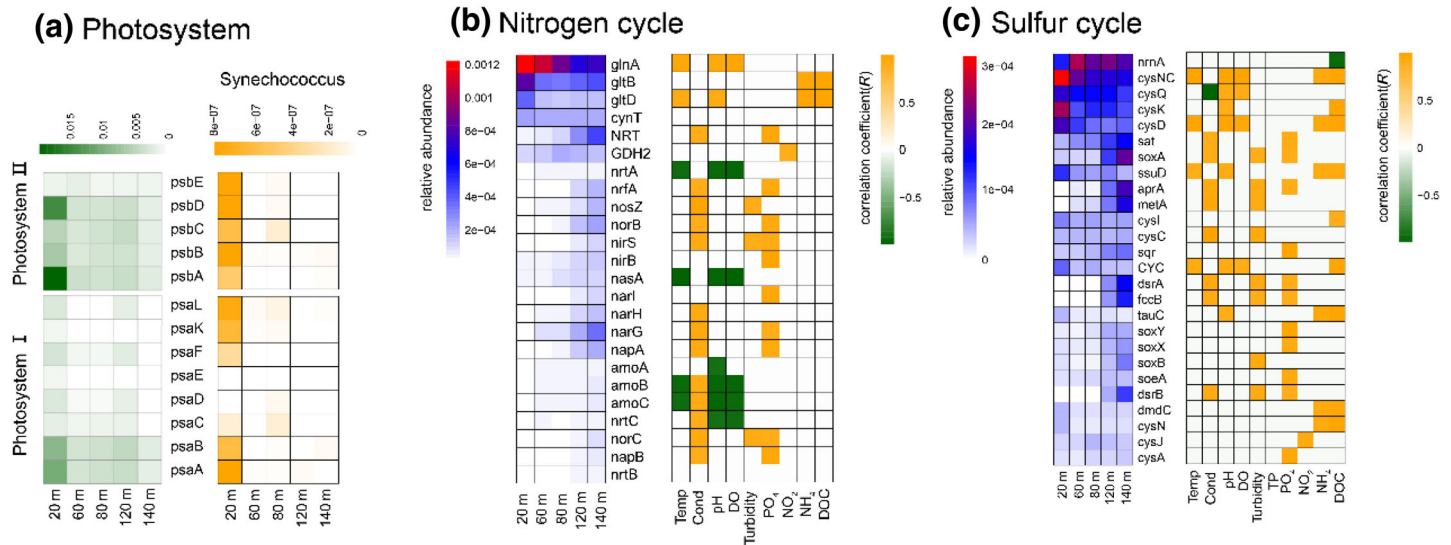


Fig. 4. Functional stratification along the depth profile. **(a)** Photosystem and major bacterial participants; **(b)** Genes involved in the nitrogen cycle ($> 1.3 \times 10^{-4}$ of normalized read assignments) and their responses to environmental factors (Pearson correlation $|R| > 0.8$ and $p < 0.05$); **(c)** Genes involved in the sulfur cycle ($> 1.7 \times 10^{-4}$ of normalized read assignments) and their responses to environmental factors (Pearson correlation $|R| > 0.8$ and $p < 0.05$).

Functional profile of the microbial communities

An average of 20.38% of the metagenomic reads could be assigned a KO number with putative functions (cutoff e-value 10^{-5}). In this study, we primarily focused on the pathways in carbon fixation, nitrogen, and sulfur cycles along the depth profile.

Photosystem

Overall, the abundances of photosystems I and II peaked at 20 m within the photic zone at the time of sampling (Fig. 4a). In addition, all of the protein subunits of photosystems I and II were present in the genus *Synechococcus* via metagenomic fragment recruitment, which coincided with their role of oxygenic photosynthesis. *Synechococcus* is supposed to be the major component of photosynthesis in the winter in Lake Fuxian. A few subunits were sparsely dispersed outside of *Synechococcus*. For example, both the D1 protein (*psbA*) and CP47 reaction center protein (*psbB*) in photosystem II were identified from *Deltaproteobacteria*.

Nitrogen cycle

Forty-six gene subfamilies targeting eight pathways in nitrogen cycle were recruited from the metagenomic reads. For ammonia fixation, both direct and indirect pathways were abundant in the lake (Fig. 4b). The ATP-dependent glutamine synthetase-encoding gene *glnA* was the most abundant nitrogen cycle gene detected, especially above a depth of 60 m. In addition, the genes *gltB* and *gltD*, encoding glutamate-oxoglutarate amidotransferase, also accumulated and can cooperate with *glnA* in indirect ammonia fixation. Glutamate dehydrogenase (GDH2 and *gdhA*) exhibited a homogeneous distribution along the depth profile, and this enzyme can

directly fix ammonia into α -ketoglutarate in an Nicotinamide adenine dinucleotide phosphate, reduced (NADPH)-dependent reaction. Glutamate synthase *gltBD* exhibited a synchronous decrease with respect to the decreasing NH₄-N concentration, whereas the presence of *gdhA* exhibited the opposite trend.

Processes such as nitrate transport, denitrification, and nitrification intensified in the deep hypolimnion. When mapping all 46 gene families in the nitrogen cycle, the abundances of *narGH*, *norZ*, *nrtABC*, and *amoABC* significantly increased along the depth profile (Supporting Information Fig. S6). Among the assayed environmental factors, DO exhibited a significant interaction with a specific set of genes. For example, the abundances of *nifH* and *amoBC* increased with the decrease in DO along the depth profile (Supporting Information Table S2). In addition, 11 out of 46 nitrogen cycle-related genes showed a positive correlation with the PO₄-P concentration along the depth profile.

Sulfur cycle

All of the functional genes involved in three steps of dissimilatory sulfate reduction (DSR), namely, the conversion (activation) of sulfate to adenosine 5'-phosphosulfate (APS, *sat*), the reduction of APS to sulfite (*aprAB*), and the reduction of sulfite to sulfide (*dsrAB*) were significantly correlated with the PO₄-P increasing profile along the depth (Supporting Information Fig. S6, Fig. 4c). The assimilatory sulfate reduction, which shares the first step with dissimilatory reduction, was synchronously strengthened, since an accumulation of *sat* was observed in the deep layers. All of the key enzymes in the Sox system were detected, with the abundance of the gene *soxA*, a subunit of SoxXA, observed at levels sixfold higher in

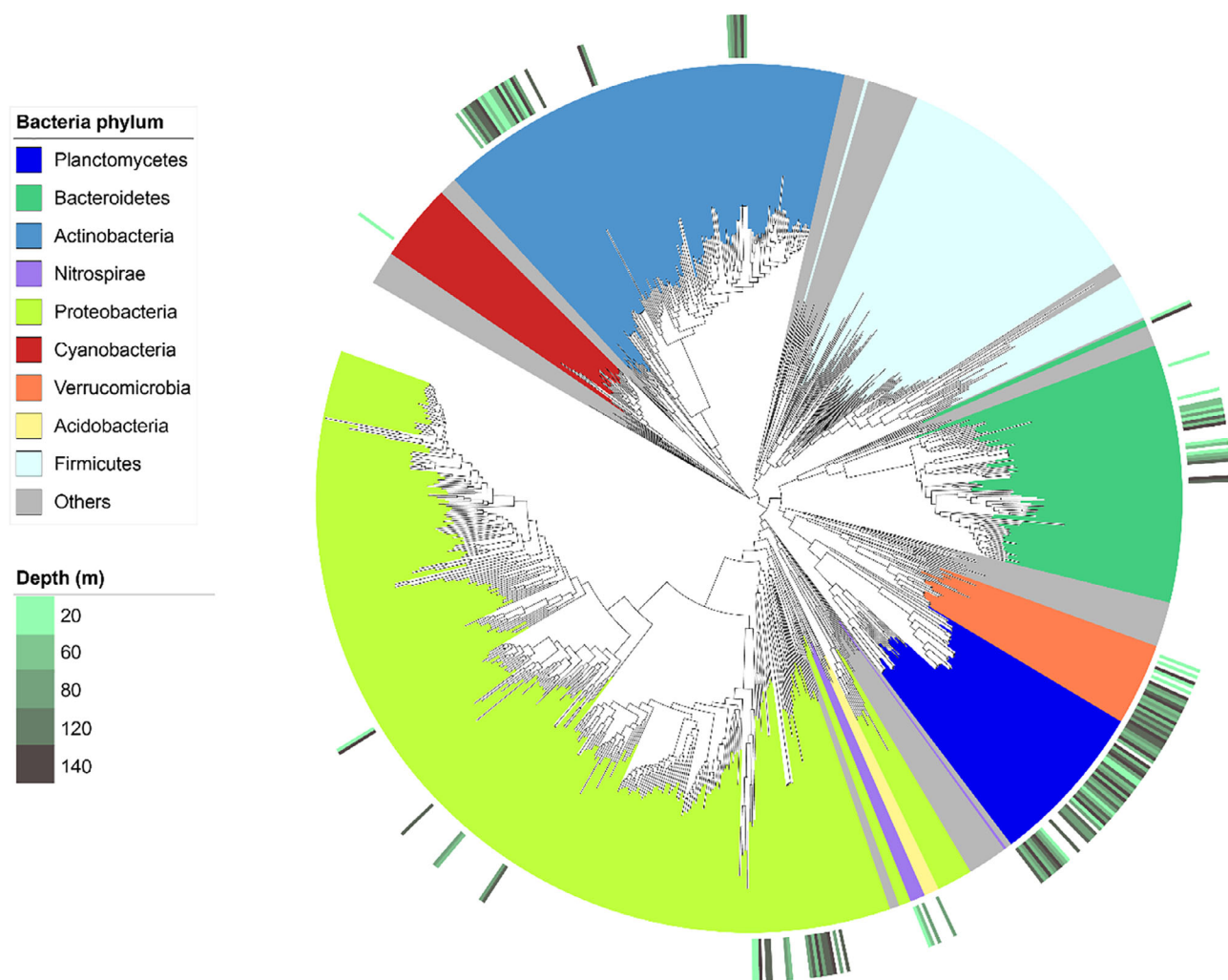


Fig. 5. Phylogeny of bacterial MAGs and their associated depths. **(a)** Maximum likelihood phylogenomic tree reconstructed by adding the reconstructed MAGs from this study (161 MAGs with completeness $\geq 80\%$ and contamination $\leq 10\%$ are shown) to the built-in tree of life in PhyloPhlAn. The outer circle indicates the distribution of MAGs among the samples; **(b)** Major vertical distribution of phyla based on MAGs; **(c)** NMDS of MAG clusters based on normalized counts of COGs in the genomes.

the deep hypolimnion than in the epilimnion (Supporting Information Table S3). On the contrary, the ATP sulfurylase genes *cysD* and *cysN* in the primary sulfate transport complex of *Mtb*, as well as the *cysC* gene that encodes APS kinase (in *Mtb*, *cysC* is fused to *cysN*, yielding a bifunctional *cysNC* gene) was induced by the accumulated DOC in the epilimnion. Similar, not only the enzyme designated *DmdA* which catalyzes the Dimethylsulfoniopropionate (DSMP) demethylation reaction producing methylmercaptopropionate (MMPA), but also a series of three coenzymes *DmdB*, *DmdC*, and *DmdD* which further metabolize MMPA were abundant in the epilimnion.

Affiliation of MAGs from Lake Fuxian

A total of 1002 MAGs were obtained from the five metagenomic data sets. After performing additional data curation, 440 MAGs (104,619 contigs, 1203.63 Mb, 11.5 kb average

contig length) met our “high quality” criteria (completeness $\geq 50\%$, contamination $\leq 10\%$, number of contigs ≤ 500) and had an average coverage depth of higher than fivefold over 90% of the nucleotides (ensuring a high confidence in base identification). The recovered MAGs spanned 10 phyla, including *Proteobacteria* (98 MAGs), *Actinobacteria* (93), *Planctomycetes* (84), *Verrucomicrobia* (38), *Bacteroidetes* (34), *Nitrospirae* (9), *Crenarchaeota* (9), *Euryarchaeota* (6), *Acidobacteria* (4), and *Cyanobacteria* (1). In addition, 64 MAGs could not be assigned to any known bacterial phylum (Supporting Information Table S4). One hundred sixty-one MAGs (completeness $\geq 80\%$, contamination $\leq 10\%$) were shown in PhyloPhlAn tree of bacteria (153 MAGs, Fig. 5a) and archaea (8 MAGs, Supporting Information Fig. S9).

The detected bacterial phyla were differentially distributed among the layers (Fig. 5b). For example, one *Cyanobacterial* MAG that was further assigned to *Synechococcus* was only

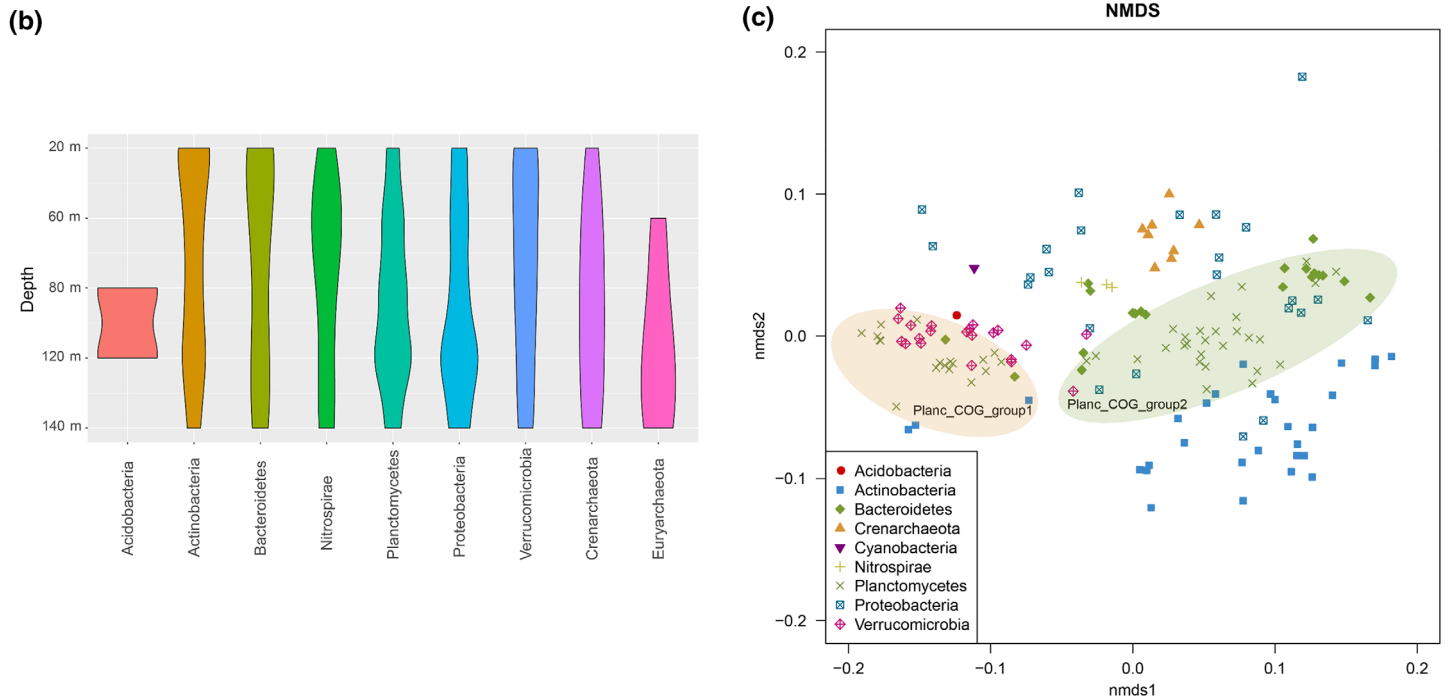


Fig. 5. Continued

identified in the epilimnion, whereas the phylum *Nitrospirae* was more abundant in the epilimnion-hypolimnion transition area. *Acidobacteria* only accumulated in the median depth of the hypolimnion (80–120 m), whereas *Planctomycetes* and *Euryarchaeota* were primarily distributed in the deep hypolimnion.

Planctomycetes diversity and Candidatus new class

The evolutionary relationships and the taxonomic ranks of the 84 *Planctomycetes* MAGs were investigated through phylogenomic analysis (Supporting Information Table S5). A maximum likelihood tree (360 *Planctomycetes*-specific genes) was constructed based on all of the single genomes and metagenomics-recovered representatives published by Andrei et al. (2019) (Fig. 6). Thirty-two MAGs clustered with the newly nominated family *Nemodlikiaceae* (CL500-3), expanding this clade from 22 to 54 MAGs, with five MAGs occurred within the new families *Vodnikaceae* and *Nixeaceae*, respectively (Supporting Information Fig. S10). Excluding the known taxa, a few MAGs formed deep branches within other clades, suggesting distinct potential genomic signatures associated with a specific habitats. Moreover, a monophyletic group with 16 MAGs was distinct from the three known clades anammox *Planctomycetes*, classes *Planctomycetacia* and *Phycisphaerae*. A new class “Plancto_FXH1” was nominated based on the bootstrap value and ANI similarity. For the novel class “Plancto_FXH1,” the 16S rRNA genes from four out of the 16 MAGs were used to anchor the new clade into the 16S rRNA gene-based phylogenetic analysis, where the MAGs fell within a new clade (Supporting

Information Fig. S11a). In addition, an entire canonical *nar* operon (*narGHJ*) was discovered from four MAGs in the new clade, which has far less similarity (ca. 30% similarity) with the two nearest reference genomes (Supporting Information Fig. S11b).

MAGs COG profile

The broad phylogenetic representation of MAGs allowed us to compare the functional potential between taxonomic groups in this ecosystem. NMDS based on normalized counts of functional genes grouped the MAG clusters according to their phylogeny, excepted for *Proteobacteria* and *Planctomycetes* (Fig. 5c). Forty-six *Planctomycetes* MAGs were divided into two groups, Planc_COG_group1 (27 MAGs), containing class *Phycisphaerae* and new nominated class “Plancto_FXH1,” and Planc_COG_group2 (19 MAGs), containing all the MAGs belong to class *Planctomycetacia* and four additional unclassified *Planctomycetes*. The estimated genome size of Planc_COG_group1 (median 2.76 Mb) was significantly smaller than that of Planc_COG_group2 (median 6.41 Mb) (Welch’s *t*-test $p < 0.001$). When checking the COG categories, only seven categories demonstrated no significant divergence between the groups, including “A RNA processing and modification,” “D Cell cycle control, cell division, chromosome partitioning,” “E Amino acid transport and metabolism,” “G Carbohydrate transport and metabolism,” “H Coenzyme transport and metabolism,” “L Replication, recombination and repair,” and “V Defense mechanisms” (Welch’s *t*-test $p > 0.05$). Interestingly, all of the

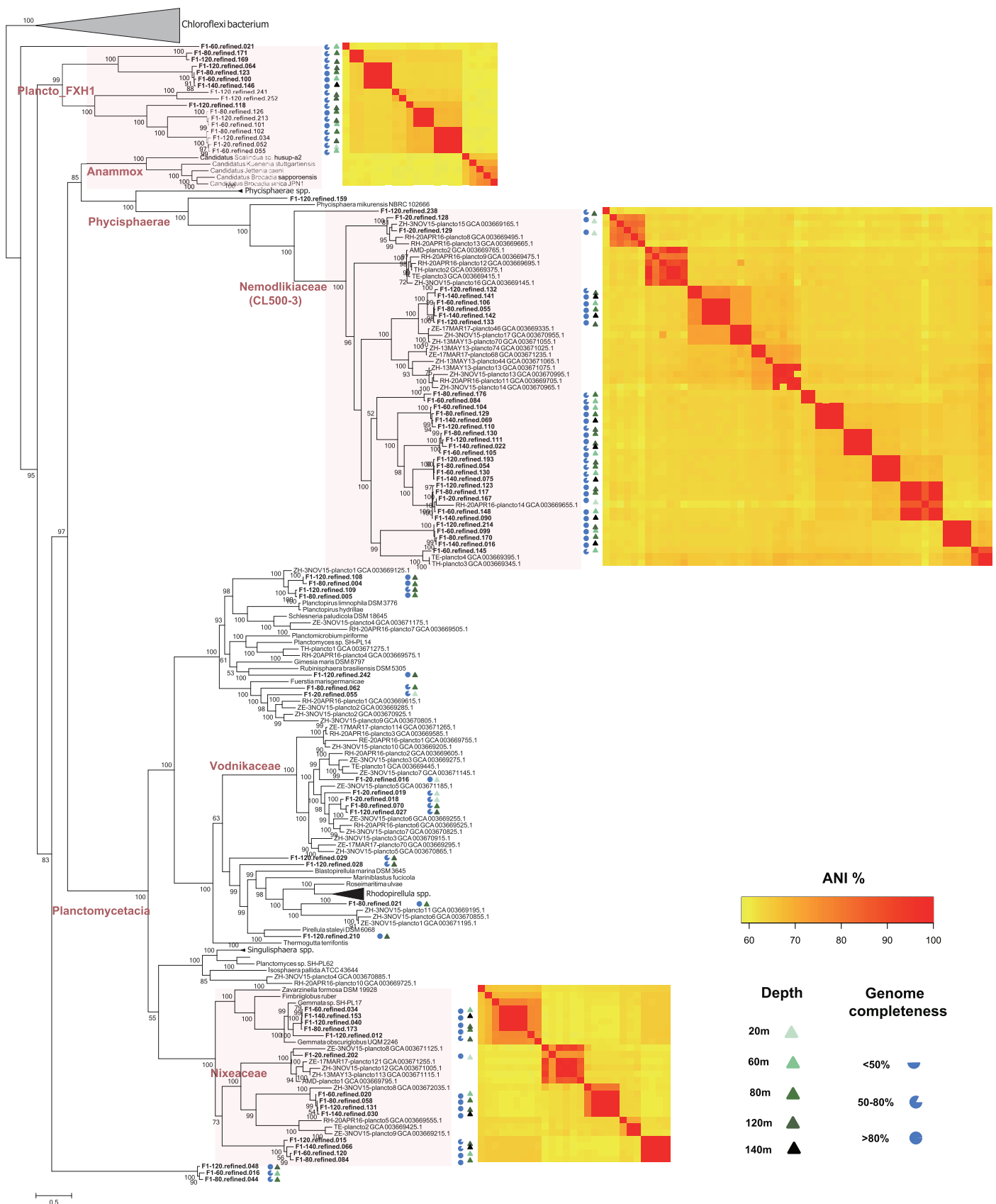


Fig. 6. Legend on next page.

core genome functions were conserved despite large variations in genome size.

Discussion

Deep lakes provide a variety of niches for microbiomes

Using a deep sequencing strategy, the results of this study provided an extensive examination of the microbial profile during the annual mixing period in Lake Fuxian. A large number of high-quality MAGs was generated to evaluate the composition and function of the microbial community. The current data set encompassed by far the largest compilation of genomic information available for several freshwater lineages, especially for the phyla *Planctomycetes* and *Verrucomicrobia*, which belong to the PVC Superphylum (Wagner and Horn 2006). Both the number of high-quality MAGs and the assembly efficiency were ubiquitous among freshwater metagenomic studies. For example, 38 *Verrucomicrobia* MAGs were produced from five metagenomes compared to the data set assembly involving 19 *Verrucomicrobia* draft genomes from 184 metagenomes collected from a eutrophic lake and a humic bog across multiple years (He et al. 2017).

Planctomycetes are ubiquitous bacteria that dwell in many types of habitats but are understudied in freshwater lakes despite being able to provide important ecosystem functions. A few typical freshwater planctomycetal clades (CL500-3, CL500-15, and CL500-37) were nominated years ago (Urbach et al. 2001), but a description of these clades typically stopped at their numerical abundances and phylogenetic diversity. Another bottleneck is a lack of representative axenic cultures for ecophysiological studies. Of 32 validly described planctomycetal species, only three species were isolated from lake water. The study of freshwater *Planctomycetes* has greatly benefited from the advent of next-generation sequencing technologies. Sixty freshwater MAGs branched within two existing classes (*Planctomycetacia* and *Phycisphaerae*). Some of the smallest freshwater *Planctomycetes* genomes have formed new freshwater-specific clades. In this work, we further contributed 84 “high-quality” MAGs to the freshwater *Planctomycetes* collection. In Lake Fuxian, the estimated genome size of phylum *Planctomycetes* distributed in a wide range, which indicated cells with large (max. 10.11 Mb) and small genome size (min. 1.98 Mb) coexisted in a habitat with a variety of niches. Although the genome size differed by more than fivefold, core genome metabolism, such as “E Amino acid transport and metabolism,” “G Carbohydrate transport and metabolism,” and “H Coenzyme transport and metabolism” remained constant. If genome streamlining represents an adaptive evolution from sediment/soil transition to aquatic environments (Andrei et al. 2019), the relative large genomes may

indicate massive gene equipment in environments where resources are scarce but diverse and where there is little penalty for slow growth (Konstantinidis and Tiedje 2005), such as the hypolimnion of deep lakes.

The life strategy of *Planctomycetes* is hot research topic in cell biology and ecology (Fuerst and Sagulenko 2011). The production of secondary metabolites that act as antimicrobials may be one solution to compete with faster growing heterotrophic bacteria. In contrast, a unique cell plan provides a distinct way for free-living *Planctomycetes* to obtain scarce resource (Wiegand et al. 2018). The results of the latest comprehensive studies indicate the existence of an exceptionally enlarged periplasmic space in planctomycetal cells (Boedeker et al. 2017), where entire high-molecular weight polysaccharides can be transported into their enlarged periplasm. This strategy would allow for the slow degradation of diverse and complex substrates in the sheltered environment of the periplasmic space without the need to secrete a plethora of different enzymes. The giant genomes we identified in Lake Fuxian provide evidence that slow growth was also successful in actual competitions.

In this work, based on the assembled MAGs, we were able to identify a monophyletic group formed by 16 MAGs that is distinct to the three known clades anammox, *Planctomycetacia* and *Phycisphaerae*. The evidence of a complete canonical *nar* operon (*narGHJK*) with a major facilitator superfamily (MFS) transporter in the new clade may provide a mechanism of surviving in the oxygen-depleted hypolimnion. Anaerobic microbial processes, reactions using oxidized compounds other than oxygen (e.g., nitrate or sulfate) as an electron acceptor, allow microbes to persist in the absence of oxygen. Furthermore, members of the phylum *Planctomycetes* have seldom been linked to denitrification and/or dissimilarity nitrate reduction, except in one case where *Kuenenia stuttgartiensis* cells were shown to reduce ammonia via nitrate to nitrite as the intermediate (Kartal et al. 2007). The newly identified clade sheds light on the function of *Planctomycetes* in the hypolimnion, not only with respect to recalcitrant carbon digestion but also in the nitrogen cycle. This new freshwater *Planctomycetes* group in denitrification could have been overlooked in previous traditional screening of denitrifying bacterial diversity. Further isolation of strains belong to this new *Planctomycetes* branch will be helpful for understanding its ecology and physiology at large.

Stratification of microbiomes has occurred since the unvarnished epilimnion-hypolimnion during the holomictic period

This study captured the phenomenon of stratification during the holomictic period of microorganisms in Lake Fuxian with

Fig. 6 Phylogeny of the *Planctomycetes*-reconstructed MAGs. Maximum likelihood phylogenomic tree reconstructed by adding the complete genomes and all available MAGs from known *Planctomycetes* and reconstructed MAGs from this study with completeness $\geq 80\%$ (shown in boldfaces) to the built-in tree of life in PhyloPhlAn. An asterisk next to an MAG indicates the presence of 16S rRNA. Bootstrap values (%) > 50 are indicated at the base of each node. An ANI comparison heat map for MAGs of each cluster is shown to the right of the clusters. Three ANI plots were made for the “Plancto_FXH1” plus anammox clade, family *Nemodlikiaceae*, and the expanded family *Nixeaceae*. Legends for depths assayed, completeness and a color key for ANI values are shown at the bottom right.

respect to both structure and function. The results obtained by metagenomics and 16S rRNA gene amplicon analyses can be mutually supported in the structure dynamics along the assayed depth profile. Measurements of environmental factors indicated that the electron acceptors such as NO₃-N increased significantly at the bottom of the lake. Meanwhile, Lake Fuxian has an unusual geological background, as the run-off from the surrounding mountains carries large quantities of sulfur into the waters (sulfur concentration in some inlets reaches 37.6 mg L⁻¹; Cai et al. 2002). In terms of electron acceptors, chemoorganoheterotrophic can oxidize many different types of organic compounds by transferring electrons from organic compounds to nitrate or sulfate when oxygen is limited, which helps in the degradation of organic materials in the hypolimnion (Knossow et al. 2015; Wenk et al. 2016). The analysis of functional genes and metabolic pathways also supported this hypothesis. A significant increase in the abundance of DSR processes was observed in the bottom water layer. Other processes such as nitrate reduction and denitrification were also activated in the hypolimnion (Llorens-Mares et al. 2015). Combined with the decreased DO in situ, we speculated on the important role of anaerobic respiration in the degradation of complex organic matters.

In contrast to the trend in the decrease of oxygen, TP and PO₄-P were accumulated in the hypolimnion that further contributes to oxygen depletion. The hypolimnetic microorganisms grow well under conditions with sufficient dissolvable phosphorus. For example, many of the nitrogen cycle-related genes were observed to have a significantly positive reaction with the increasing PO₄-P in the hypolimnion. In those anoxic environments, fermenting bacteria extracted energy from large organic molecules. The resulting smaller compounds, such as fatty acids and alcohols, were further oxidized by acetogens, methanogens, and the competing sulfate-reducing microorganisms (Nakagawa et al. 2012; Bush et al. 2017; Linz et al. 2018). Thus the fermentative short-chain fatty acids can be used as the carbon sources to enhance the biological phosphorus removal under the anoxic condition (Tong and Chen 2007). Moreover, with the hypolimnetic phosphorus escaping to epilimnion during the vertical mixing, a positive feedback system can be generated in phytoplankton and provide more autochthonous organic matter down to the hyperlimnion that further contributes to oxygen depletion (Kim et al. 2006; Hamilton et al. 2010).

Hypolimnetic oxygen concentration has long been considered to be an important indicator of environmental changes (Müller et al. 2012), since the demand of oxygen in the hypolimnion probably increases during eutrophication. If sufficient amounts of oxygen cannot be supplied to the lake bottom during mixing, the oxygen minimum zone may be extended during the subsequent water stable stratification. A number of hypolimnetic macroorganisms will be either lost or forced into the epilimnion. The hypoxia developed have led to local reduction of mesozooplankton prey in these regions

(Vanderploeg et al. 2009). Changes in the structure of food web as well as the microbial loop may further control the microbial community. Moreover, the initial disappearance of oxygen in the hypolimnion can occur prior to any noticeable changes in the productivity of phytoplankton in the epilimnion since the remineralization of organic epilimnetic input by the sediments (Pjevac et al. 2015). The oxygen content of the hypolimnion and the rate of disappearance constitutes a potential “early warning system” of changes in the lake trophic state.

Conclusion

In this study, we focused on microbial community composition and function in the hypolimnetic layers during the vertical mixing. The results indicated that advances in sequencing depth and bioinformatics strategy was highly useful for describing the depth profile of microbiomes associated with the environmental changes. The anaerobic respiration with nitrate and sulfate as the terminal electron acceptors were accumulated at bottom of hypolimnion, from where the anaerobic phosphate release was transported to the epilimnion thereby providing a potentially significant internal source of phosphorus. The present data set of 440 MAGs encompasses by far the largest compilation of genomic information available for many freshwater lineages. The new class “Plancto_FXH1” of *Planctomycetes* with a distinct nitrate reduction operon shed light on the function and strategy of “less abundant phyla” in the oxygen-deficient hypolimnion. Furthermore, targeted enrichment and cultivation of microbes would be helpful in solving open questions behind metagenomic analysis, which is important to the association between biogeochemical cycles and their microbial participants.

References

- Alneberg, J., and others. 2014. Binning metagenomic contigs by coverage and composition. *Nat. Methods* **11**: 1144–1146. doi:10.1038/nmeth.3103
- Andrei, A.-Ş., M. M. Salcher, M. Mehrshad, P. Rychtecký, P. Znachor, and R. Ghai. 2019. Niche-directed evolution modulates genome architecture in freshwater *Planctomycetes*. *ISME J.* **13**: 1056–1071. doi:10.1038/s41396-018-0332-5
- Boedeker, C., and others. 2017. Determining the bacterial cell biology of *Planctomycetes*. *Nat. Commun.* **8**: 14853. doi:10.1038/ncomms14853
- Bolger, A. M., M. Lohse, and B. Usadel. 2014. Trimmomatic: A flexible trimmer for Illumina sequence data. *Bioinformatics* **30**: 2114–2120. doi:10.1093/bioinformatics/btu170
- Bush, T., M. Diao, R. J. Allen, R. Sinnige, G. Muyzer, and J. Huisman. 2017. Oxic-anoxic regime shifts mediated by feedbacks between biogeochemical processes and microbial community dynamics. *Nat. Commun.* **8**: 789. doi:10.1038/s41467-017-00912-x

- Cabello-Yeves, P. J., R. Ghai, M. Mehrshad, A. Picazo, A. Camacho, and F. Rodriguez-Valera. 2017. Reconstruction of diverse verrucomicrobial genomes from metagenome datasets of freshwater reservoirs. *Front. Microbiol.* **8**: 2131. doi:10.3389/fmicb.2017.02131
- Cai, L., C. K. M. Tsui, K. Q. Zhang, and K. D. Hyde. 2002. Aquatic fungi from Lake Fuxian, Yunnan, China. *Fungal Divers.* **9**: 57–70. doi:10.1017/S0953756202005658
- Danis, P. A., U. von Grafenstein, V. Masson-Delmotte, S. Planton, D. Gerdeaux, and J. M. Moisselin. 2004. Vulnerability of two European lakes in response to future climate changes. *Geophys. Res. Lett.* **31**: L21507. doi:10.1029/2004GL020833
- Denef, V. J., R. S. Mueller, E. Chiang, J. R. Liebig, and H. A. Vanderploeg. 2015. *Chloroflexi* CL500-11 populations that predominate deep-lake hypolimnion bacterioplankton rely on nitrogen-rich dissolved organic matter metabolism and C1 compound oxidation. *Appl. Environ. Microbiol.* **82**: 1423–1432. doi:10.1128/AEM.03014-15
- Fu, L., B. Niu, Z. Zhu, S. Wu, and W. Li. 2012. CD-HIT: Accelerated for clustering the next-generation sequencing data. *Bioinformatics* **28**: 3150–3152. doi:10.1093/bioinformatics/bts565
- Fuerst, J. A., and E. Sagulenko. 2011. Beyond the bacterium: *Planctomycetes* challenge our concepts of microbial structure and function. *Nat. Rev. Microbiol.* **9**: 403–413. doi:10.1038/nrmicro2578
- Greenberg, A., L. Clesceri, and A. Eaton. 1992. Standard methods for the examination of water and wastewater, 18th ed. American Public Health Association.
- Hamilton, D. P., K. R. O'Brien, M. A. Burford, J. D. Brookes, and C. G. McBride. 2010. Vertical distributions of chlorophyll in deep, warm monomictic lakes. *Aquat. Sci.* **72**: 295–307. doi:10.1007/s00027-010-0131-1
- He, S., S. L. R. Stevens, L. K. Chan, S. Bertilsson, T. Glavina Del Rio, S. G. Tringe, R. R. Malmstrom, and K. D. McMahon. 2017. Ecophysiology of freshwater *Verrucomicrobia* inferred from metagenome-assembled genomes. *mSphere* **2**: e00277–e00217. doi:10.1101/150078
- Henson, M. W., V. C. Lanclos, B. C. Faircloth, and J. C. Thrash. 2018. Cultivation and genomics of the first freshwater SAR11 (LD12) isolate. *ISME J.* **12**: 1846–1860. doi:10.1038/s41396-018-0092-2
- Huerta-Cepas, J., K. Forslund, L. P. Coelho, D. Szklarczyk, L. J. Jensen, C. von Mering, and P. Bork. 2017. Fast genome-wide functional annotation through orthology assignment by eggNOG-mapper. *Mol. Biol. Evol.* **34**: 2115–2122. doi:10.1093/molbev/msx148
- Hyatt, D., P. F. Locascio, L. J. Hauser, and E. C. Uberbacher. 2012. Gene and translation initiation site prediction in metagenomic sequences. *Bioinformatics* **28**: 2223–2230. doi:10.1093/bioinformatics/bts429
- Kanehisa, M., Y. Sato, and K. Morishima. 2016. BlastKOALA and GhostKOALA: KEGG tools for functional characterization of genome and metagenome sequences. *J. Mol. Biol.* **428**: 726–731. doi:10.1016/j.jmb.2015.11.006
- Kang, D. D., J. Froula, R. Egan, and Z. Wang. 2015. MetaBAT, an efficient tool for accurately reconstructing single genomes from complex microbial communities. *PeerJ* **3**: e1165. doi:10.7717/peerj.1165
- Kartal, B., M. M. Kuypers, G. Lavik, J. Schalk, H. J. Op den Camp, M. S. Jetten, and M. Strous. 2007. Anammox bacteria disguised as denitrifiers: Nitrate reduction to dinitrogen gas via nitrite and ammonium. *Environ. Microbiol.* **9**: 635–642. doi:10.1111/j.1462-2920.2006.01183.x
- Kim, C., Y. Nishimura, and T. Nagata. 2006. Role of dissolved organic matter in hypolimnetic mineralization of carbon and nitrogen in a large, monomictic lake. *Limnol. Oceanogr.* **51**: 70–78. doi:10.4319/lo.2006.51.1.0070
- Kimura, M. 1980. A simple method for estimating evolutionary rates of base substitutions through comparative studies of nucleotide sequences. *J. Mol. Evol.* **16**: 111–120. doi:10.1007/BF01731581
- Knossow, N., B. Blonder, W. Eckert, A. V. Turchyn, G. Antler, and A. Kamyshny Jr. 2015. Annual sulfur cycle in a warm monomictic lake with sub-millimolar sulfate concentrations. *Geochem. Trans.* **16**: 7. doi:10.1186/s12932-015-0021-5
- Konstantinidis, K. T., and J. M. Tiedje. 2005. Towards a genome-based taxonomy for prokaryotes. *J. Bacteriol.* **187**: 6258–6264. doi:10.1128/JB.187.18.6258-6264.2005
- Kumar, S., G. Stecher, and K. Tamura. 2016. MEGA7: Molecular evolutionary genetics analysis version 7.0 for bigger datasets. *Mol. Biol. Evol.* **33**: msw054. doi:10.1093/molbev/msw054
- Lagesen, K., P. F. Hallin, E. Rødland, H. H. Stærfeld, T. Rognes, and D. W. Ussery. 2007. RNAMmer: Consistent and rapid annotation of ribosomal RNA genes. *Nucleic Acids Res.* **35**: 3100–3108. doi:10.1093/nar/gkm160
- Lavoie, M., and J. C. Auclair. 2012. Phosphorus mobilization at the sediment–water interface in softwater shield lakes: The role of organic carbon and metal oxyhydroxides. *Aquat. Geochem.* **18**: 327–341. doi:10.1007/s10498-012-9166-3
- Lewis, W. M., Jr. 1983. A revised classification of lakes based on mixing. *Can. J. Fish. Aquat. Sci.* **40**: 1779–1787. doi:10.1139/f83-207
- Li, D., R. Luo, C. Liu, C. Leung, H. Ting, K. Sadakane, H. Yamashita, and T. Lam. 2016. MEGAHIT v1.0: A fast and scalable metagenome assembler driven by advanced methodologies and community practices. *Methods* **102**: 3–11. doi:10.1016/j.ymeth.2016.02.020
- Lindström, E. S., K. Vrede, and E. Leskinen. 2004. Response of a member of the *Verrucomicrobia*, among the dominating bacteria in a hypolimnion, to increased phosphorus availability. *J. Plankton Res.* **26**: 241–246. doi:10.1093/plankt/fbh010
- Linz, A. M., B. C. Crary, A. Shade, S. Owens, J. A. Gilbert, R. Knight, and K. D. McMahon. 2017. Bacterial community composition and dynamics spanning five years in freshwater bog lakes. *mSphere* **2**: e00169–e00117. doi:10.1128/mSphere.00169-17

- Linz, A. M., S. He, S. L. Stevens, K. Anantharaman, R. R. Rohwer, R. Malmstrom, S. Bertilsson, and K. D. McMahon. 2018. Connections between freshwater carbon and nutrient cycles revealed through reconstructed population genomes. *bioRxiv*:365627. doi:[10.7717/peerj.6075](https://doi.org/10.7717/peerj.6075)
- Livingstone, D. M. 2003. Impact of secular climate change on the thermal structure of a large temperate central European lake. *Clim. Change* **57**: 205–225. doi:[10.1023/A:1022119503144](https://doi.org/10.1023/A:1022119503144)
- Llorens-Mares, T., S. Yooseph, J. Goll, J. Hoffman, M. Vila-Costa, C. M. Borrego, C. L. Dupont, and E. O. Casamayor. 2015. Connecting biodiversity and potential functional role in modern euxinic environments by microbial metagenomics. *ISME J.* **9**: 1648–1661. doi:[10.1038/ismej.2014.254](https://doi.org/10.1038/ismej.2014.254)
- Lu, J., F. P. Breitwieser, P. Thielen, and S. L. Salzberg. 2017. Bracken: Estimating species abundance in metagenomics data. *PeerJ Comput. Sci.* **3**: e104. doi:[10.7717/peerj-cs.104](https://doi.org/10.7717/peerj-cs.104)
- Matzinger, A., and others. 2007. Eutrophication of ancient Lake Ohrid: Global warming amplifies detrimental effects of increased nutrient inputs. *Limnol. Oceanogr.* **52**: 338–353. doi:[10.4319/lo.2007.52.1.0338](https://doi.org/10.4319/lo.2007.52.1.0338)
- Mehrshad, M., M. M. Salcher, Y. Okazaki, S. I. Nakano, K. Simek, A. S. Andrei, and R. Ghai. 2018. Hidden in plain sight—highly abundant and diverse planktonic freshwater *Chloroflexi*. *Microbiome* **6**: 176. doi:[10.1186/s40168-018-0563-8](https://doi.org/10.1186/s40168-018-0563-8)
- Müller, B., L. D. Bryant, A. Matzinger, and A. Wüest. 2012. Hypolimnetic oxygen depletion in eutrophic lakes. *Environ. Sci. Technol.* **46**: 9964–9971. doi:[10.1021/es301422r](https://doi.org/10.1021/es301422r)
- Naeher, S., A. Gilli, R. P. North, Y. Hamann, and C. J. Schubert. 2013. Tracing bottom water oxygenation with sedimentary Mn/Fe ratios in Lake Zurich, Switzerland. *Chem. Geol.* **352**: 125–133. doi:[10.1016/j.chemgeo.2013.06.006](https://doi.org/10.1016/j.chemgeo.2013.06.006)
- Nakagawa, M., and others. 2012. Seasonal change in microbial sulfur cycling in monomictic Lake Fukami-ike, Japan. *Limnol. Oceanogr.* **57**: 974–988. doi:[10.4319/lo.2012.57.4.0974](https://doi.org/10.4319/lo.2012.57.4.0974)
- Neuenschwander, S. M., R. Ghai, J. Pernthaler, and M. M. Salcher. 2018. Microdiversification in genome-streamlined ubiquitous freshwater Actinobacteria. *ISME J.* **12**: 185–198. doi:[10.1038/ismej.2017.156](https://doi.org/10.1038/ismej.2017.156)
- Ng, C., and others. 2010. Metaproteogenomic analysis of a dominant green sulfur bacterium from Ace Lake, Antarctica. *ISME J.* **4**: 1002–1019. doi:[10.1038/ismej.2010.28](https://doi.org/10.1038/ismej.2010.28)
- Okazaki, Y., and S. I. Nakano. 2016. Vertical partitioning of freshwater bacterioplankton community in a deep mesotrophic lake with a fully oxygenated hypolimnion (Lake Biwa, Japan). *Environ. Microbiol. Rep.* **8**: 780–788. doi:[10.1111/1758-2229.12439](https://doi.org/10.1111/1758-2229.12439)
- Okazaki, Y., S. Fujinaga, A. Tanaka, A. Kohzu, H. Oyagi, and S.-i. Nakano. 2017. Ubiquity and quantitative significance of bacterioplankton lineages inhabiting the oxygenated hypolimnion of deep freshwater lakes. *ISME J.* **11**: 2279–2293. doi:[10.1038/ismej.2017.89](https://doi.org/10.1038/ismej.2017.89)
- Okazaki, Y., M. M. Salcher, C. Callieri, and S. I. Nakano. 2018. The broad habitat spectrum of the CL500-11 lineage (phylum *Chloroflexi*), a dominant bacterioplankton in oxygenated hypolimnia of deep freshwater lakes. *Front. Microbiol.* **9**: 2891. doi:[10.3389/fmicb.2018.02891](https://doi.org/10.3389/fmicb.2018.02891)
- Parks, D. H., M. Imelfort, C. T. Skennerton, P. Hugenholtz, and G. W. Tyson. 2015. CheckM: Assessing the quality of microbial genomes recovered from isolates, single cells, and metagenomes. *Genome Res.* **25**: 1043–1055. doi:[10.1101/gr.186072.114](https://doi.org/10.1101/gr.186072.114)
- Pjevac, P., M. Korlevic, J. S. Berg, E. Bura-Nakic, I. Ciglenecki, R. Amann, and S. Orlic. 2015. Community shift from phototrophic to chemotrophic sulfide oxidation following anoxic holomixis in a stratified seawater lake. *Appl. Environ. Microbiol.* **81**: 298–308. doi:[10.1128/AEM.02435-14](https://doi.org/10.1128/AEM.02435-14)
- Rabalais, N. N., D. E. Harper, and R. E. Turner. 2001. Responses of nekton and demersal and benthic fauna to decreasing oxygen concentrations, p. 115–128. *In* N. N. Rabalais and R. E. Turner [eds.], *Coastal hypoxia: Consequences for living resources and ecosystems. Coastal and estuarine studies*, v. **58**. American Geophysical Union.
- Roux, S., F. Enault, B. L. Hurwitz, and M. B. Sullivan. 2015. VirSorter: Mining viral signal from microbial genomic data. *PeerJ* **3**: e985. doi:[10.7717/peerj.985](https://doi.org/10.7717/peerj.985)
- Salcher, M. M., J. Pernthaler, N. Frater, and T. Posch. 2011. Vertical and longitudinal distribution patterns of different bacterioplankton populations in a canyon-shaped, deep prealpine lake. *Limnol. Oceanogr.* **56**: 2027–2039. doi:[10.4319/lo.2011.56.6.2027](https://doi.org/10.4319/lo.2011.56.6.2027)
- Salcher, M. M., S. M. Neuenschwander, T. Posch, and J. Pernthaler. 2015. The ecology of pelagic freshwater methylophiles assessed by a high-resolution monitoring and isolation campaign. *ISME J.* **9**: 2442–2453. doi:[10.1038/ismej.2015.55](https://doi.org/10.1038/ismej.2015.55)
- Segata, N., D. Börnigen, X. C. Morgan, and C. Huttenhower. 2013. PhyloPhlAn is a new method for improved phylogenetic and taxonomic placement of microbes. *Nat. Commun.* **4**: 2304–2304. doi:[10.1038/ncomms3304](https://doi.org/10.1038/ncomms3304)
- Song, W. Z., and T. Thomas. 2017. Binning_refiner: Improving genome bins through the combination of different binning programs. *Bioinformatics* **33**: 1873–1875. doi:[10.1093/bioinformatics/btx086](https://doi.org/10.1093/bioinformatics/btx086)
- Sorokin, D. Y., and others. 2012. Nitrification expanded: Discovery, physiology and genomics of a nitrite-oxidizing bacterium from the phylum *Chloroflexi*. *ISME J.* **6**: 2245–2256. doi:[10.1038/ismej.2012.70](https://doi.org/10.1038/ismej.2012.70)
- Tong, J., and Y. Chen. 2007. Enhanced biological phosphorus removal driven by short-chain fatty acids produced from waste activated sludge alkaline fermentation. *Environ. Sci. Technol.* **41**: 7126–7130. doi:[10.1021/es071002n](https://doi.org/10.1021/es071002n)
- Urbach, E., K. L. Vergin, L. Young, A. Morse, G. L. Larson, and S. J. Giovannoni. 2001. Unusual bacterioplankton community structure in ultra-oligotrophic Crater Lake. *Limnol. Oceanogr.* **46**: 557–572. doi:[10.4319/lo.2001.46.3.0557](https://doi.org/10.4319/lo.2001.46.3.0557)

- Uritskiy, G. V., J. DiRuggiero, and J. Taylor. 2018. MetaWRAP—a flexible pipe-line for genome-resolved metagenomic data analysis. *Microbiome* **6**: 158. doi:[10.1186/s40168-018-0541-1](https://doi.org/10.1186/s40168-018-0541-1)
- Vanderploeg, H. A., and others. 2009. Hypoxia affects spatial distributions and overlap of pelagic fish, zooplankton, and phytoplankton in Lake Erie. *J. Exp. Mar. Biol. Ecol.* **381**: S92–S107. doi:[10.1016/j.jembe.2009.07.027](https://doi.org/10.1016/j.jembe.2009.07.027)
- Wagner, M., and M. Horn. 2006. The *Planctomycetes*, *Verrucomicrobia*, *Chlamydiae* and sister phyla comprise a superphylum with biotechnological and medical relevance. *Curr. Opin. Biotechnol.* **17**: 241–249. doi:[10.1016/j.copbio.2006.05.005](https://doi.org/10.1016/j.copbio.2006.05.005)
- Wang, S., and H. Dou. 1998. China lakes chorography. Science Press, [in Chinese].
- Wenk, C. B., and others. 2016. Differential N₂O dynamics in two oxygen-deficient lake basins revealed by stable isotope and isotopomer distributions. *Limnol. Oceanogr.* **61**: 1735–1749. doi:[10.1002/lno.10329](https://doi.org/10.1002/lno.10329)
- Wetzel, R. G. 2001. *Limnology: Lake and river ecosystems*, 3rd ed. Academic Press.
- Wiegand, S., M. Jogler, and C. Jogler. 2018. On the maverick *Planctomycetes*. *FEMS Microbiol. Rev.* **42**: 739–760. doi:[10.1093/femsre/fuy029](https://doi.org/10.1093/femsre/fuy029)
- Wood, D. E., and S. L. Salzberg. 2014. Kraken: Ultrafast metagenomic sequence classification using exact alignments. *Genome Biol.* **15**: R46. doi:[10.1186/gb-2014-15-3-r46](https://doi.org/10.1186/gb-2014-15-3-r46)
- Wu, Y. W., Y. H. Tang, S. G. Tringe, B. A. Simmons, and S. W. Singer. 2014. MaxBin: An automated binning method to recover individual genomes from metagenomes using an expectation-maximization algorithm. *Microbiome* **2**: 26. doi:[10.1186/2049-2618-2-26](https://doi.org/10.1186/2049-2618-2-26)

Acknowledgments

We would like to thank Wenlei Luo and Qinghua Liu for their help in the field sampling organization. This work was funded by National Natural Science Foundation of China (31722008), Science & Technology Basic Resources Investigation Program of China (2017FY100300), National Natural Science Foundation of China (31730013, 91751111), Chinese Academy of Sciences (QYZDJ-SSW-DQC030), and the Youth Innovation Promotion Association of CAS (2014273).

Conflict of Interest

None declared.

Submitted 27 January 2019

Revised 21 June 2019

Accepted 05 September 2019

Associate editor: David Walsh